Reversal in spreading of a tabbed circular jet under controlled excitation

K. B. M. Q. Zaman and G. Raman[a)]
NASA Lewis Research Center, Cleveland, Ohio 44135

(Received 14 February 1997; accepted 22 August 1997)

Detailed flow field measurements have been carried out for a turbulent circular jet perturbed by tabs and artificial excitation. Two "delta tabs" were placed at the nozzle exit at diametrically opposite locations. The excitation condition involved subharmonic resonance that manifested in a periodic vortex pairing in the near flow field. While the excitation and the tabs independently increased jet spreading, a combination of the two diminished the effect. The jet spreading was most pronounced with the tabs but was reduced when excitation was applied to the tabbed jet. The tabs generated streamwise vortex pairs that caused a lateral spreading of the jet in a direction perpendicular to the plane containing the tabs. The excitation, on the other hand, organized the azimuthal vorticity into coherent ring structures whose evolution and pairing also increased entrainment by the jet. In the tabbed case, the excitation produced coherent azimuthal structures that were distorted and asymmetric in shape. The self-induction of these structures produced an effect that opposed the tendency for the lateral spreading of the streamwise vortex pairs. The passage of the distorted vortices, and their pairing, also had a cancellation effect on the time-averaged streamwise vorticity field. These led to the reduction in jet spreading. [S1070-6631(97)03012-2]

I. INTRODUCTION

In a continuing effort to increase mixing in free shear flows, vortex generators in the form of tabs have been researched by several investigators in recent years.[1–6] A tab is a small protrusion into the flow, which, with appropriate geometry, produces a counter-rotating streamwise vortex pair that can impact the flow downstream significantly. The streamwise vortices usually have a long life and, once introduced in the flow, tend to persist over tens of jet diameters downstream. This is in contrast to azimuthal vortical structures that are more energetic but have a shorter life span. The generation mechanism of the streamwise vortex pairs by the tabs and their effect on the entrainment and spreading of free jets have been discussed, e.g., in Refs. 4–7.

The azimuthal or spanwise component of vorticity, on the other hand, constitutes almost all of the vorticity shed initially in jets and mixing layers. This subsequently rolls up into large-scale coherent structures that continually interact and evolve to larger sizes with increasing distance downstream. The profound role of the coherent structures in mixing layer dynamics is well recognized through numerous previous studies (e.g., Refs. 8 and 9). It is also well known that one can manipulate these coherent vortical structures and their dynamics through controlled excitation, at least in the initial region of the mixing layer, which, in turn, can have a significant impact on the entrainment and spreading of the flow downstream (e.g., Refs. 9–11). For example, excitation inducing "subharmonic resonance" had been observed to cause a large increase in jet spreading (Ref. 12). Subharmonic resonance in the present context refers to excitation with a fundamental and a smaller-amplitude subharmonic component, which, under appropriate conditions, would cause a transfer of energy leading to a very large growth of the subharmonic (for an analysis of the phenomenon see, e.g., Refs. 13 and 14). Physically, the process would involve pairing of vortical structures that have initially rolled up at the fundamental frequency causing halving of the passage frequency of the dominant structures (Refs. 10, 15, and 16).

During the course of the study reported in Ref. 12, the influence of subharmonic resonance was briefly investigated for a tabbed jet. Since such excitation and the tabs independently increased jet spreading, the expectation was that a suitable combination might increase the spreading even more. The unpublished results, however, indicated an opposite effect. The centerline mean velocity decay for the circular jet under consideration increased when the excitation was applied. It increased even more when two tabs, designed after Ref. 1, were used. But when the excitation was applied to the tabbed jet the decay was not as much as that observed simply with the tabs.

The primary purpose of the present experiment was to investigate and try to explain this "anomalous" effect. This was deemed feasible because of the advances, over the past years, in the understanding of the flow field over a tab and the development of experimental procedures for measurement of the vorticity field.[17] The objective was to carry out measurements in an attempt to understand the vorticity dynamics that led to the effect. An additional purpose of the investigation was to gain some insight into mechanisms by which certain flow resonances, e.g., in jets impinging on a collector or in screeching supersonic jets, were suppressed by the tabs.[1,4] Even though these resonance phenomena were complex, involving feedback loops, it was felt that an understanding of the vorticity dynamics in the presence of the tabs might shed some light in that direction.

[a)]With NYMA, Inc., NASA Lewis Group.

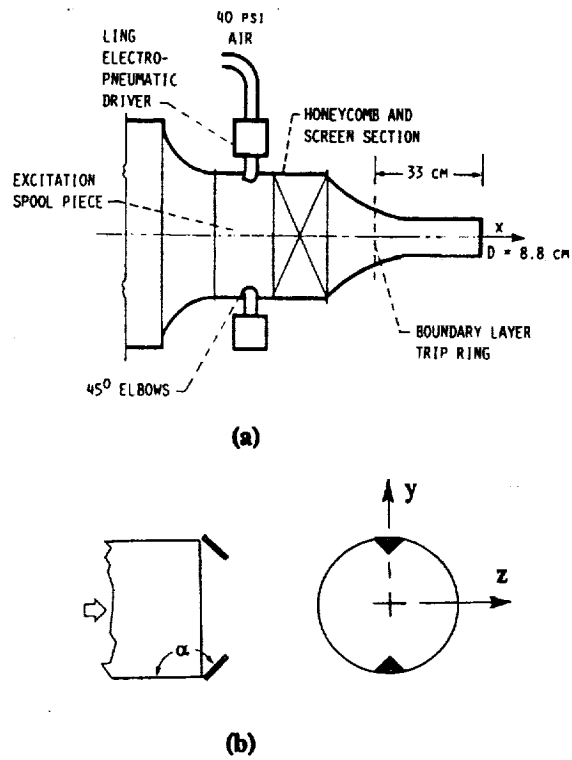

FIG. 1. Schematic of the jet facility: (a) Nozzle and excitation device, (b) tab configuration.

II. EXPERIMENTAL METHOD

The experiment was carried out in a free jet facility having a 76 cm diam plenum chamber.[12,17] Essentially the same configuration described in Ref. 12 was used. The nozzle, with a diameter, $D=8.8$ cm, and the excitation apparatus are shown schematically in Fig. 1(a). Two electropneumatic (Ling) drivers were used to impart the excitation. Plenum chamber resonant frequencies were utilized in order to achieve large amplitudes that were required to produce the effect under consideration.

The mass flow required to run the Ling drivers also constituted the supply for the jet flow. The flow conditioning unit yielded a top-hat profile at the exit of the nozzle. Unfortunately, a "clean" jet flow could not be achieved with this arrangement; the turbulence intensity at the nozzle exit center was measured to be about 2%. The requirement for achieving a high level of excitation conflicted with that for achieving a "clean" jet flow. A superimposed primary flow, together with the Ling driver flow, would improve the flow quality, but at the expense of the maximum available excitation amplitude. Similarly, adding more screens in the flow conditioning unit would also reduce the turbulence as well as the excitation amplitude. On the other hand, reducing the size of the jet (Reynolds number and Mach number) would provide a higher excitation amplitude together with a cleaner flow; but this would be realized at the expense of probe resolution required in the measurements. Thus, the flow and the excitation conditions were chosen as a compromise and these are described further in the following.

A wave form synthesizer produced the excitation function comprised of a fundamental ($f_F=530$ Hz) and its subharmonic ($f_{F/2}=265$ Hz). The corresponding Strouhal numbers, based on jet diameter (D) and velocity (U_J), were 0.62 and 0.31. This wave form drove the Ling drivers to produce rms fundamental and subharmonic amplitudes of $u'_F/U_J=0.026$ and $u'_{F/2}/U_J=0.015$, measured at the jet exit. The phase between the fundamental and the subharmonic, although not critical at these high amplitudes, was chosen by trial and error to yield maximum subharmonic growth downstream.[12]

Two "delta tabs" were used, as shown in Fig. 1(b). Each had a triangular shape with the base placed on the nozzle wall and the apex leaning downstream at an angle of 135°. This tab shape, for a given area blockage, was found in earlier studies to produce the strongest effect in terms of mixing layer distortion; an explanation of why this geometry was optimum for producing the strongest streamwise vortex pair was provided in Ref. 5. The tab sizes were chosen such that the area blockage due to each was about 1.8% of the nozzle exit area. The nozzle boundary layer was turbulent, with a momentum thickness of about $0.006D$; the protruding height of the tab was much larger—about $0.1D$. Again, the tab size was chosen based on unpublished previous studies to produce an optimum increase in the jet spreading with minimum thrust loss; further enlarging of the tab increased the jet spreading at the expense of a disproportionately large thrust loss. The measurements were carried out for a jet Mach number, $M_J=0.22$, which corresponded to a Reynolds number, $\mathrm{Re}_D=450\,000$.

Standard Pitot probe and hot-wire surveys were conducted using a computer controlled probe traversing mechanism. Two X-wire probes, one in the "$u-v$" and the other in the "u-w" configuration, were traversed successively through the same grid points to obtain the three velocity components. Here, u, v, and w denote velocity components in the x, y, and z directions, respectively; the coordinate system is shown in Fig. 1. The finite separation of the sensors in the X elements introduced errors in the v and w data due to u gradients; this was corrected following published procedures.[18] The distributions of v and w in y and z yielded streamwise vorticity, $\omega_x=\partial w/\partial y-\partial v/\partial z$. Inside the core of the jet, the uncertainty in the normalized streamwise velocity was estimated to be within $\pm 1\%$, and that in the streamwise vorticity to be $\pm 20\%$. However, progressively larger errors are expected away from the core, as well as in regions of high fluctuation intensity, primarily due to flow angularity. The data shown are as measured and no correction is attempted. The overall vorticity distributions should be considered qualitative.

The subharmonic component of the excitation signal was used as a reference for phase averaging. The four hot-wire signals and the reference signal were sampled simultaneously. The phase averaging was performed on line using the peaks in the reference signal as triggers. The $\langle u\rangle$, $\langle v\rangle$, and $\langle w\rangle$ data, for 19 phases within a period, were stored for each grid point on a y-z plane. These data were postprocessed to obtain streamwise vorticity, $\langle\omega_x\rangle$. The notation $\langle f\rangle$ is used to indicate the phase average of a function f.

Whereas $\langle\omega_x\rangle$ is obtained from the actual spatial distri-

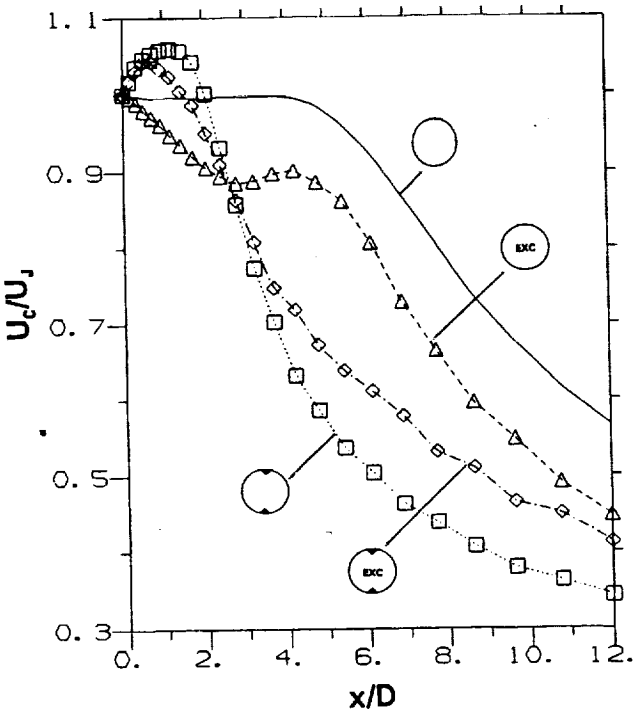

FIG. 2. Centerline variations of mean velocity.

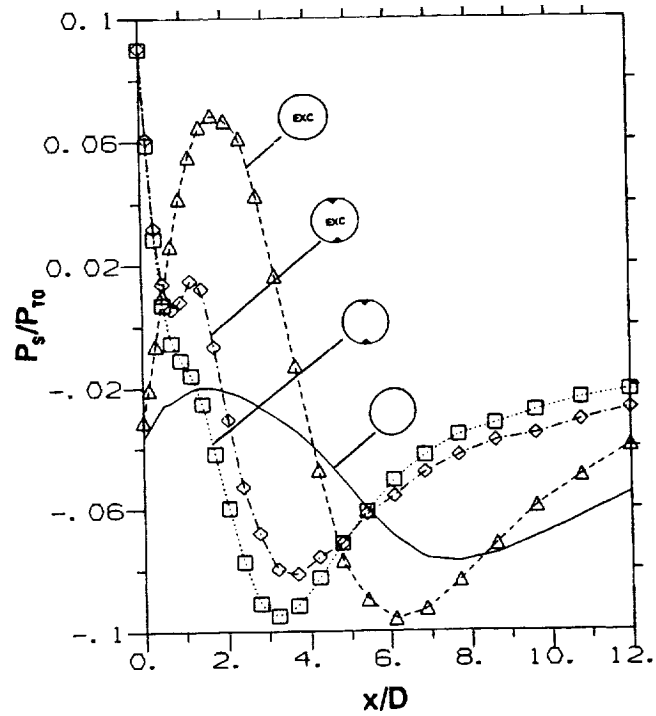

FIG. 3. Centerline variations of static pressue.

butions of $\langle v\rangle(y,z)$ and $\langle w\rangle(y,z)$, Taylor's hypothesis is invoked to estimate the components $\langle\omega_Y\rangle$ and $\langle\omega_Z\rangle$. These are calculated as $\langle\omega_Y\rangle=\partial\langle u\rangle/\partial z+(1/U_C)\partial\langle w\rangle/\partial t$, and $\langle\omega_Z\rangle=-(1/U_C)\partial\langle v\rangle/\partial t-\partial\langle u\rangle/\partial y$. Here, the notation t represents time with respect to the trigger location, and U_C is a convection velocity assumed to be $0.5U_J$. From the three components of vorticity, enstrophy, $\langle\xi\rangle=(\langle\omega_x\rangle^2+\langle\omega_Y\rangle^2+\langle\omega_Z\rangle^2)^{1/2}$ is calculated, which is the square of the magnitude of the vorticity vector. It should be noted that $\langle\omega_X\rangle$ is typically much smaller in amplitude than the azimuthal components $\langle\omega_Y\rangle$ and $\langle\omega_Z\rangle$. Thus, $\langle\xi\rangle$ essentially represents the concentration of phase-averaged, squared, azimuthal vorticity in the flow field. Further details of the measurements can be found in Ref. 17.

III. RESULTS AND DISCUSSION

Figure 2 shows the variation of the mean streamwise velocity (U_C) measured on the jet centerline. Four cases—the jet with and without tabs, each with and without excitation—are considered. In this and subsequent figures the cases for each dataset are identified by symbols that should be self-explanatory; "exc" implies the excited condition. A trend, as described in the Introduction, can be observed. While with two tabs the velocity decay is most rapid, excitation together with the tabs reduces the effect. Note that a faster centerline velocity decay indicates a larger jet spreading, although entire flow field measurements are required to make a definitive inference.

One finds that for the tab cases the flow first accelerates on the centerline. On the other hand, for the excited case a deceleration occurs. These trends are reflected in the corresponding static pressure (P_S) variations, shown in Fig. 3. Note that the total pressure can only decrease or remain constant. Corresponding total pressure variations (not shown) together with the static pressure data of Fig. 3 reasonably reproduced the hot-wire velocity data, confirming the trends observed and the accuracy of the data obtained by hot-wire anemometry. The acceleration of the flow under the effect of the tabs is expected as the flow is deflected toward the centerline. A similar trend has been documented in prior experiments on the effect of tabs (e.g., Ref. 4). However, the deceleration of the flow under the excitation is somewhat intriguing. The likely reason for this is an energy exchange from the mean flow to the growing instability waves (see, e.g., Ref. 14). Physically, the process corresponds to rolling up, and subsequent interaction, of discrete vortical structures. It is also accompanied by an increased spreading of the shear layer that is addressed further in the following.

The centerline variations of the u' spectral amplitudes are shown in Fig. 4 for the excited cases with and without tabs. The large growth of the subharmonic amplitude, or "subharmonic resonance," is physically accompanied by the pairing of vortex rings that initially roll up at the fundamental frequency.[10] One find that, even with the tabs, a substantial increase occurs in the subharmonic amplitude. The vortex pairing activity in the presence of the tabs is explored in the following.

Figure 5 shows an isosurface of the streamwise mean velocity for the four cases. The two cross-sectional cuts, for each dataset, are located at $x/D=1$ and 12. These data were obtained by Pitot probe surveys at five x stations. A visual impression of the jet spreading for each case can be obtained from these data. For the excited case without tabs, the jet "diameter" goes through a curious increase and decrease before continuing to increase. The trend depends on the cho-

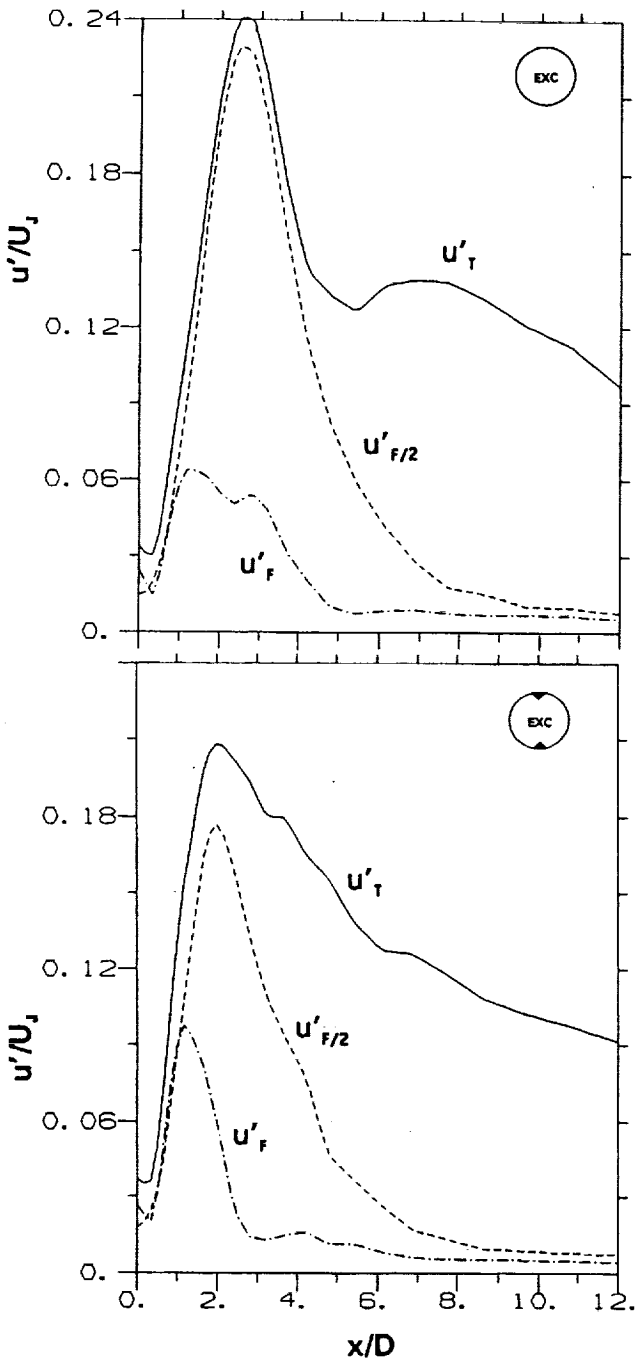

FIG. 4. Centerline variations of total, fundamental, and subharmonic amplitudes (rms) for the excited cases.

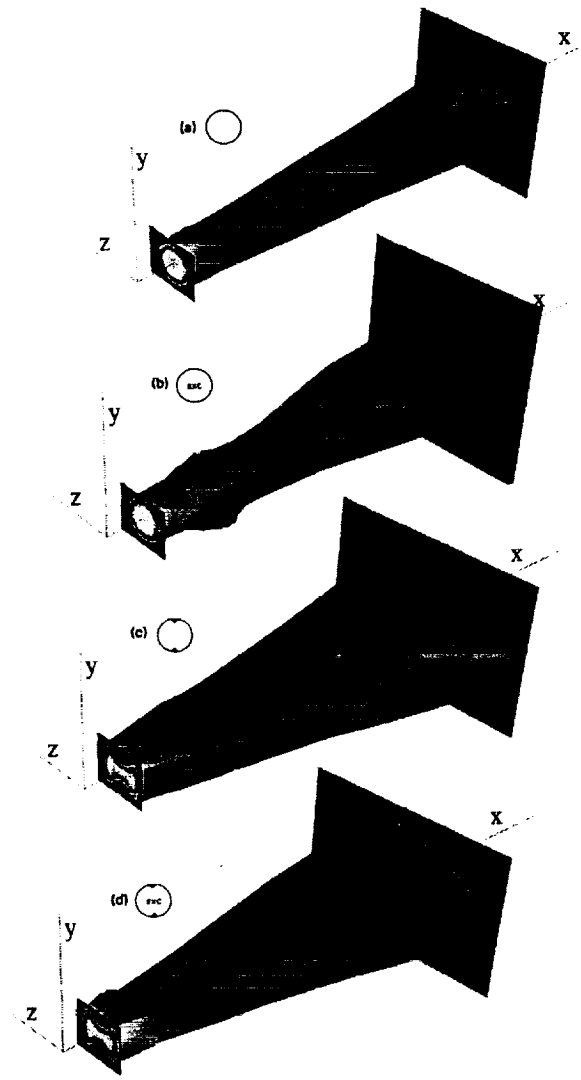

FIG. 5. The $U/U_{MAX}=0.3$ isosurface over the range $1<x/D<12$.

sen isosurface and, as will become clear from the next figure, is not in error to violate continuity. A similar trend was observed in the work reported in Ref. 10. The faster initial expansion of the jet cross section occurs as the slower moving vortex ring enlarges while the faster one pushes into it during the pairing process. Once the faster one has leapfrogged and amalgamation has ensued the outer ring apparently picks up speed and its radius collapses. This is accompanied by the shrinkage in the jet cross section. This is also the region that is marked by negative (countergradient) Reynolds stress.[10] We turn our attention to the tabbed case, however, which is the focus of the present investigation. One finds that with only the tabs the jet spreading is large. The spreading occurs in a direction perpendicular to the plane containing the tabs. This lateral spreading can be seen to have reduced considerably when the excitation is applied.

The streamwise variations of the normalized mass flux ($\dot{m}$), obtained by integration of the Pitot probe survey data, for the four cases are shown in Fig. 6; the data have been normalized by the initial mass flux of the jet ($\dot{m}_J$). The results for the unexcited, no-tab case are in good agreement with published data (e.g., Ref. 9). The excited case data, without tabs, are also similar in trend with the data for "preferred mode" excitation reported in Ref. 9. The fluxes for the tab cases are clearly higher. One also finds, confirming the inference drawn from the centerline velocity data (Fig. 2), that the overall spreading in the downstream regions is indeed reduced when the excitation is applied to the tabbed jet.

Time-averaged streamwise vorticity distributions for the tab cases are shown in Fig. 7, based on measurements at $x/D=1$, 1.5, 2.3, and 4. Two isosurfaces, representing equal and opposite amplitudes, are shown. As viewed from downstream, the yellow (lighter) and red (darker) regions repre-

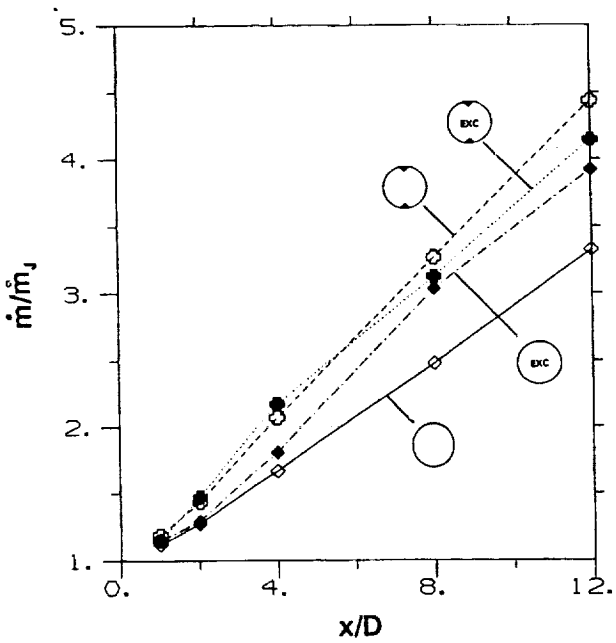

FIG. 6. Variations of streamwise mass flow rates with x/D.

sent counterclockwise and clockwise rotations, respectively. Thus, each tab has produced a pair of counter-rotating vortices with an "in-flow" sense of rotation so as to ingest ambient fluid into the core of the jet. For the unexcited case, it should be apparent that these vortices have rearranged and formed two "out-flow" pairs, which, with increasing distance downstream, have spread in the lateral (z) direction. The induced motion of the out-flow vortex pairs is the primary mechanism by which the spreading of the jet takes place under the influence of the tabs.[17] It should also be clear from Fig. 7 that the excitation has impacted the ω_x field quite significantly. The lateral spreading of the vortices (in the z direction) has been reduced noticeably. Also, two additional pairs of vortices have appeared on the lateral edges under the excitation.

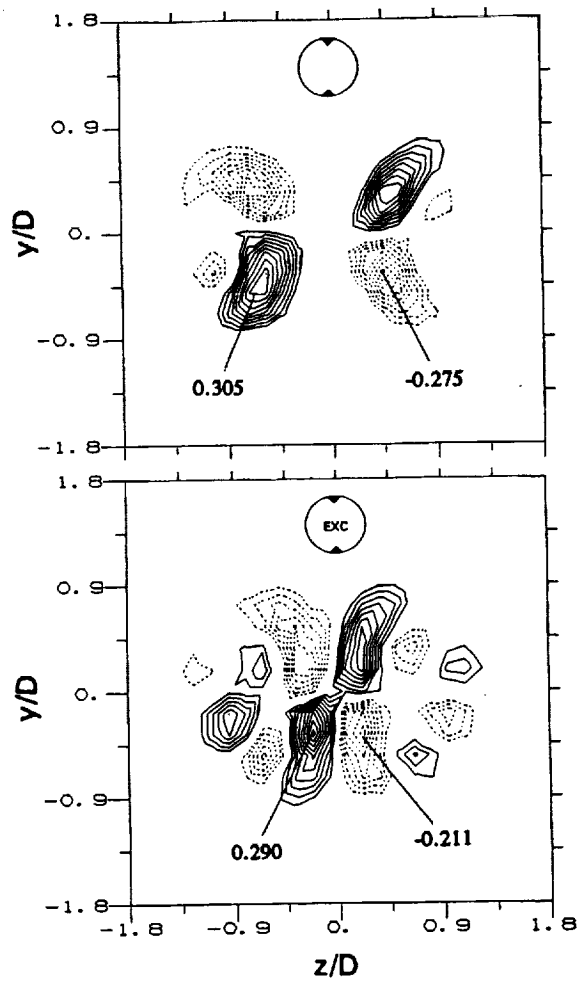

FIG. 8. Mean streamwise orticity, $\omega_X D/U_J$, at $x/D=3$.

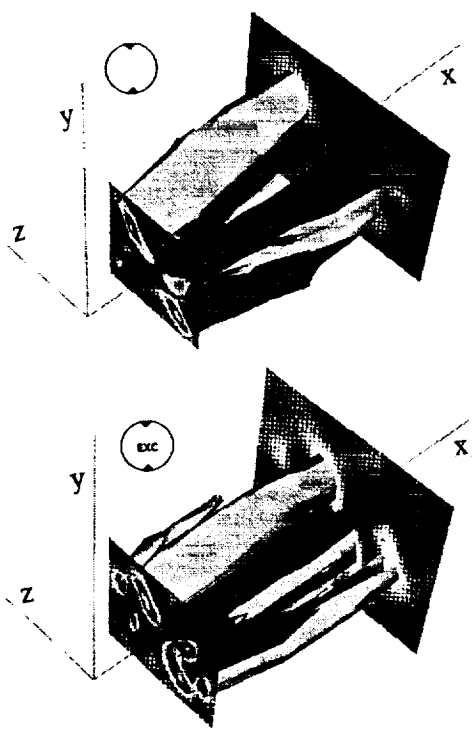

FIG. 7. Mean streamwise vorticity, over $1<x/D<4$, shown by isosurfaces, $\omega_X D/U_J=0.1$ (red) and -0.1 (yellow).

A clearer comparison of the ω_X field with and without excitation is made in Fig. 8, with data for $x/D=3$, as an example. The contour plots show that not only has the lateral spreading of the streamwise vortices been reduced but also the amplitudes have dropped somewhat. What causes these effects on the streamwise vorticity field is the essential question under consideration in this paper. An answer is sought through phase-averaged measurements of the vorticity field.

Distributions of phase-averaged streamwise vorticity $\langle\omega_X\rangle$ are shown in Fig. 9 for four phases (ϕ), as examples. The data are for the excited case with the tabs at $x/D=3$. The phases chosen are approximately at equal intervals within the subharmonic period. It is clear that the streamwise vorticity distribution goes through dramatic changes within the period, and the dynamics are vigorous; note that a complete reversal in the sign of the vortex pairs takes place with varying phase. The changes in the $\langle\omega_X\rangle$ distribution with

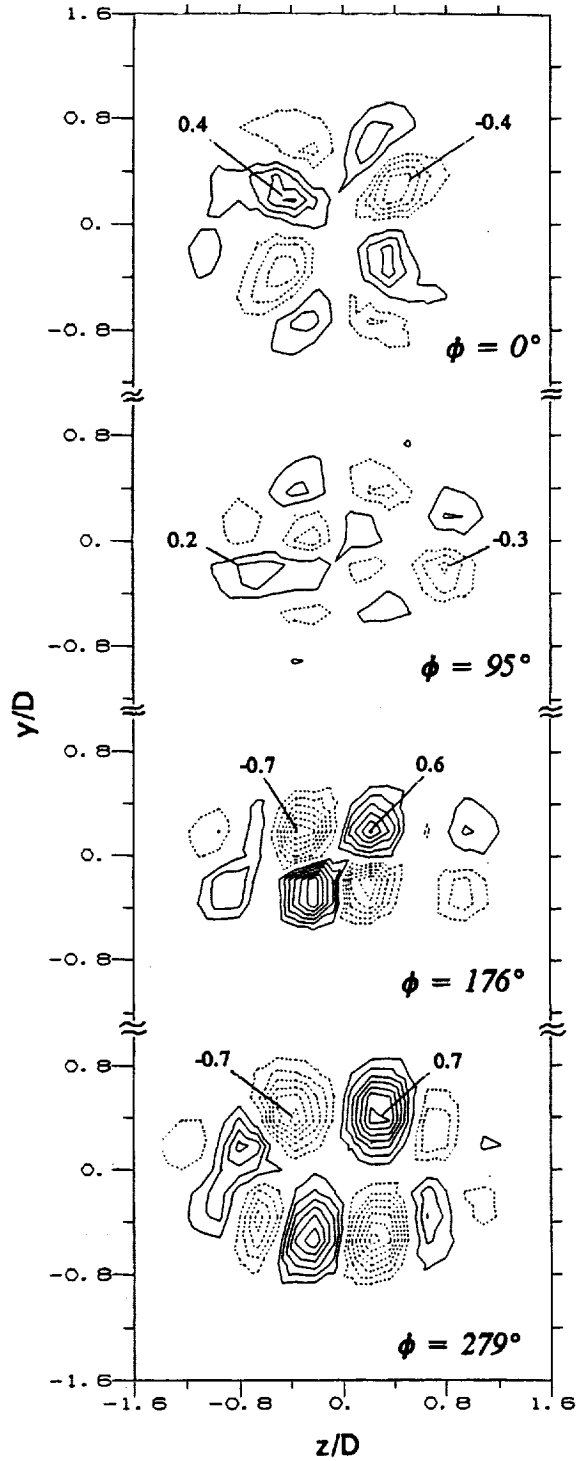

FIG. 9. Phase-averaged streamwise vorticity, $\langle \omega_X \rangle D/U_J$, at $x/D=3$ for indicated phases.

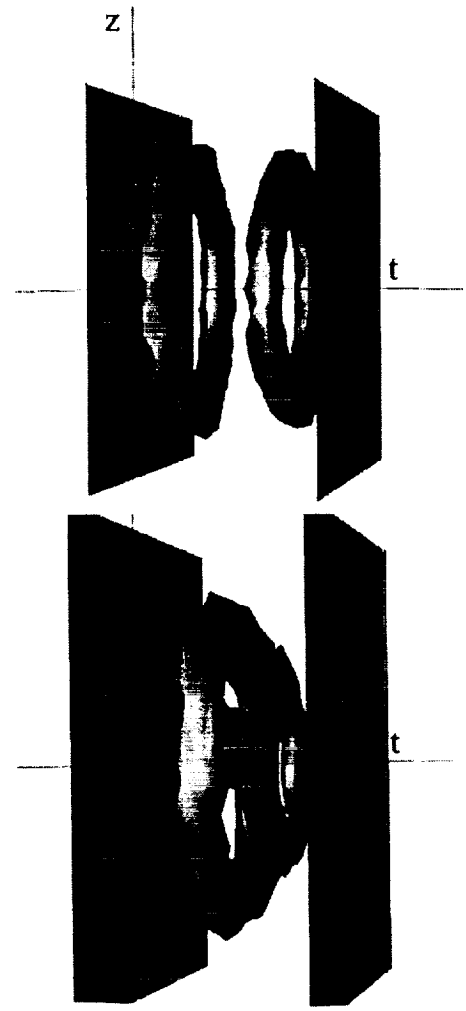

FIG. 10. Phase-averaged enstrophy isosurfaces for the excited case without tabs. Top figure: $x/D=1$, $\langle \xi \rangle D/U_J=6.0$. Bottom figure: $x/D=2$, $\langle \xi \rangle D/U_J=4.0$.

phase, and also in the time-averaged ω_X field, are due to the dynamics and interaction of the azimuthal vorticity, which have rolled up into concentrated, periodic, coherent structures by the excitation. In the tabbed case, these structures are distorted and asymmetric in shape. The passage of these structures leaves a footprint, even on the time-averaged field, because their evolution is also a function of space. This becomes clear with the $\langle \xi \rangle$ data.

First, Fig. 10 shows the time variation of an isosurface of $\langle \xi \rangle$ for the excited case without tabs. The data show variation on the y-z plane as a function of phase (time) covering the full period of the subharmonic, and are for $x/D=1$ (top) and $x/D=2$ (bottom). With an appropriate choice of the isosurface level, $\langle \xi \rangle$ vividly displays the concentration of the azimuthal vorticity within the flow field. The two vortex rings undergoing the pairing process are clearly captured by the data. The phase-averaging process has smoothed out any incoherent, three-dimensionality that might have accompanied the pairing process. Such three-dimensionality, manifesting azimuthal instability, are typically observed in flow visualization studies of vortex pairing (see, e.g., Ref. 19). Note in Fig. 10 that positive t represents negative x, and thus, the vortex rings can be thought of as traveling from the right to the left. The view in the lower picture, therefore, represents a condition just prior to the pairing (and not after a leapfrogging of the inner ring). Data at $x/D=3$ and 4 basically show a single vortex ring after the completion of pairing; these are not shown, again, because the focus here is on the tab case.

Corresponding enstrophy data for the excited case with the tabs are shown in Fig. 11. In order to capture the essence

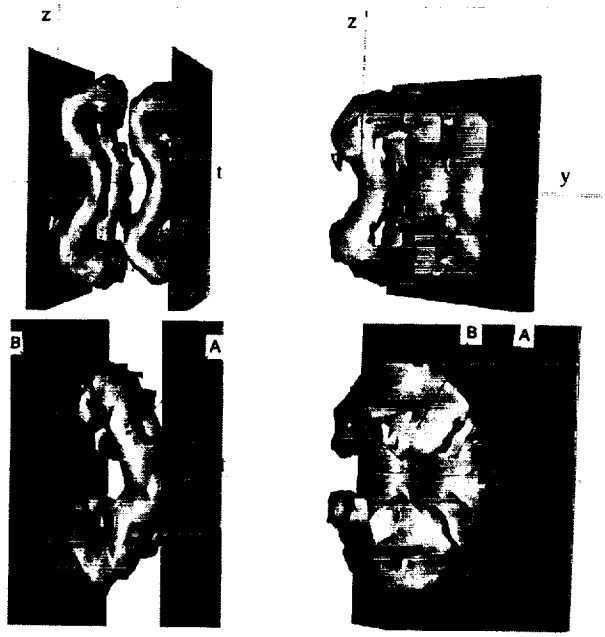

FIG. 11. Phase-averaged enstrophy isosurfaces for the excited case with tabs. Top: $x/D=1$, $\langle\xi\rangle D/U_J=4.0$. Bottom: $x/D=3$, $\langle\xi\rangle D/U_J=1.6$. Figures on right are another view of the same data as on the left.

of the complex vortex interaction, data are presented for $x/D=1$ and 3, with two views for each x station. It becomes clear that each of the vortex rings has gone through large distortions before the pairing, as seen in the views on the top ($x/D=1$).

At $x/D=3$, pairing has occurred, but in a manner that is far more complex than that observed in the no-tab case. Here, the inner segments of the vortical structures, seen at $x/D=1$, have amalgamated to form the bowed elliptical structure on the right (marked as A). The distorted tips of the vortices, on either end of the z axis, have broken away and amalgamated to form two ring structures on the left (marked as B). These ring structures are connected to the elliptical structure at the top and bottom. In the lower right picture, the left plane of the measurement domain has truncated the two ring structures, creating the appearance of four stretched out limbs. An inspection reveals that the streamwise vorticity associated with the four limbs is of the same sense as that of the tab vortices. The periodic passage of the four stretched out limbs has apparently produced the two additional vortex pairs identified in Fig. 7.

The pairing process for the tab case is further examined with data at $x/D=1.5$, shown in Fig. 12. On the top are two views [(a) and (b)] of enstrophy distribution as in Fig. 11. A similar pattern as observed at $x/D=1$ can be seen, except that the pairing is at a more advanced stage. It should be apparent that each structure has curled inward (in z). This is expected from the self-induction of a distorted vortex, and the process causes a squeezing of the jet cross section in the z direction. In other words, the rolled up structures are asymmetric initially with the long axis aligned with the z direction. From mechanisms governing axis switching, it is known that each of these vortices, while propagating downstream, would shrink in the direction of its major (z) axis while expanding in the direction of the minor (y) axis (see, e.g., Refs. 17, 20–22). Now recall from an earlier discussion (Fig. 7) that the streamwise vortices produced by the tabs tend to expand laterally in the z direction. Thus, with the excitation imparted to the tabbed jet, the azimuthal vorticity

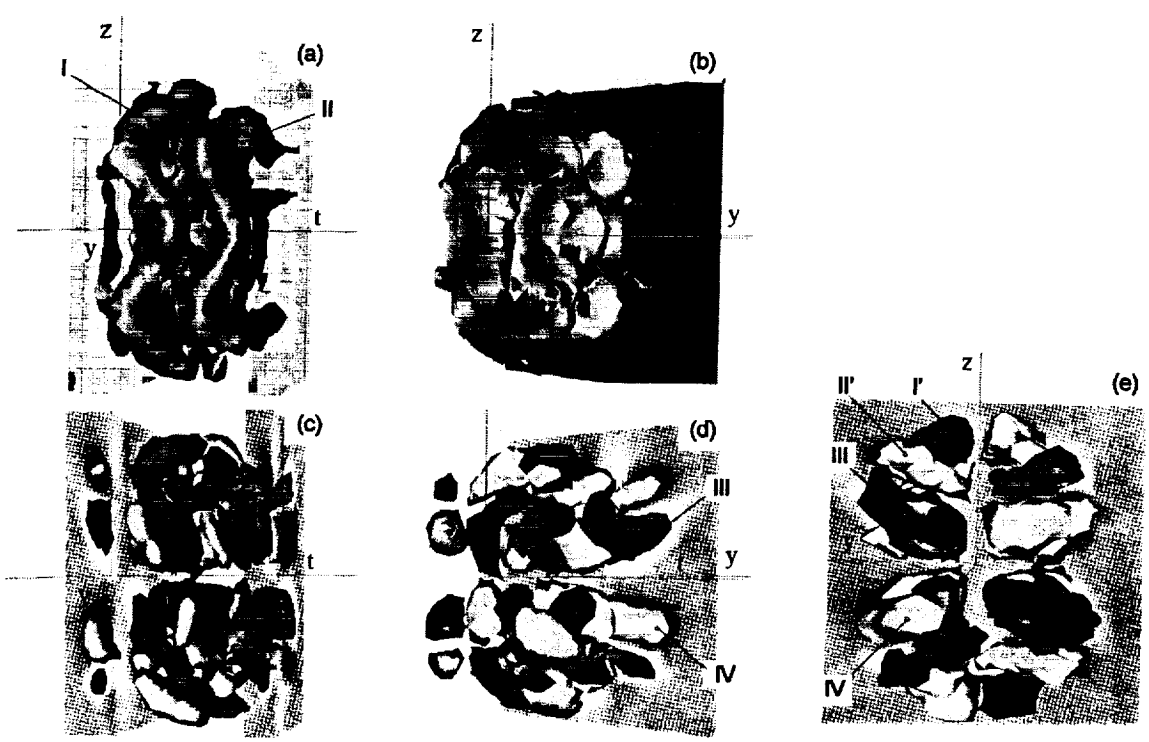

FIG. 12. Phase-averaged data at $x/D=1.5$: (a) and (b) are two views of the isosurface, $\langle\xi\rangle D/U_J=3.0$; (c), (d), and (e) are three views of $\langle\omega_x\rangle D/U_J=+0.5$ (red) and -0.5 (yellow).

rolls up into the distorted structures, whose dynamics then oppose the tendency for the lateral spreading in the z direction. This is thought to be the primary mechanism by which the spreading of the jet is inhibited.

For the mechanism described in the previous paragraph, pairing may not be necessary. Even though it was not explored in detail, it is expected that excitation at a single frequency (e.g., at the "preferred mode," as in Ref. 9) would also result in a similar reduction in the lateral spreading of the jet from a circular nozzle fitted with two tabs. One may also speculate that there would be a similar reduction in the spreading of a circular jet fitted with more of a number of equally spaced tabs, because a similar, albeit more complex, self-induction of the vortex structures would be operative. The role of vortex pairing in the present context is not completely clear. However, it may have accentuated the effect. This is because the pairing process results in a shrinkage of the faster moving vortex [one on the right in Fig. 12(a)], further squeezing the jet cross section in the z direction.

The chosen isosurface levels in Figs. 10 and 11, for $x/D=1$, should make it apparent that the vorticity is less intense in the tabbed case (the peak value of $\langle\xi\rangle D/U_J$ in the measurement domain dropped from 16.6 in the no-tab case to 12.2 in the tabbed case). In other words, the coherent structures in the tabbed case are not only distorted but are also weaker. These two factors are thought to play a role in the mechanism by which flow resonance, e.g., screech in supersonic jets, is suppressed by the tabs. The aeroacoustics of these resonance phenomena involve impingement of the coherent vortical structures on an obstacle (on standing shock waves in the case of screech); the resultant noise feeds back to the nozzle lip to initiate the formation of new coherent structures, completing the feedback loop. Vortical structures attaining higher intensity (i.e., higher peak vorticity) and having better azimuthal uniformity, prior to the interaction with the obstacle, may be expected to be more efficient in sustaining the process. With the insertion of tabs, the vortical structures suffer on both counts, thus rendering the process less effective or ineffective.

Referring back to Fig. 12(a), inspection should reveal that segments of the vortex on the left, identified as I, amalgamate with corresponding segments from the vortex on the right to produce the "ring structures" (and the "stretched out limbs") discussed earlier in Fig. 11. Segments identified as II curl inward and apparently disappear by $x/D=3$. These latter segments have a streamwise vorticity component with a sense opposite that of the tab vortices. Diffusion of these has most likely reduced the strength of the tab vortices.

Phase-averaged streamwise vorticity, $\langle\omega_X\rangle$, data are shown in Figs. 12(c) and 12(d), with the same viewing angles as in (a) and (b). The distributions are complex; in addition to vorticity from the tabs, the reorientation of the azimuthal vortices has obviously contributed to this field. A scrutiny identifies the "tab vortices" that are marked III and IV in (d). This becomes clearer from another view of the same data shown in Fig. 12(e). This view, in the streamwise direction, yields a perspective of the time-averaged field such as seen in Fig. 8. The additional vortices on either end of the z axis have apparently occurred due to the reorientation of the azimuthal vorticity shown in Figs. 12(a) and 12(b). Specifically, segments marked I′ and II′ in (e) have occurred due to a contribution from segments I and II in (a). Thus, the inward curling of the azimuthal vortical structures has not only squeezed in the "tab vortices" but also reduced their strength by diffusing streamwise vorticity of the opposite sense.

IV. CONCLUDING REMARKS

The effect of excitation inducing vortex pairing in a tabbed jet has been investigated. While the tabs and the excitation independently increase the spreading of the jet, a combination of the two reduces the effect. The reduced jet spreading is traced to an inward curling of the coherent azimuthal vortices organized by the excitation. The inward curling is caused by self-induction of the distorted azimuthal vortices. This squeezes the jet cross section in a direction in which the streamwise vortex pairs from the tabs tend to spread. In other words, the dynamics of the excitation induced azimuthal vortices conflict with the spreading tendency of the "tab vortices." Parts of the reoriented azimuthal vorticity also has a sense opposite to that of the tab vortices, which apparently causes a reduction in the strength of the latter through diffusion. The measured vorticity distributions thus provide a qualitative explanation for the observed reduction of jet spreading when excitation is applied to a tabbed jet.

[1]K. K. Ahuja and W. H. Brown, "Shear flow control by mechanical tabs," AIAA Paper No. 89-0994, 1989.

[2]P. Surks, C. B. Rogers, and D. E. Parekh, "Entrainment and acoustic variations in a round jet from introduced streamwise vorticity," AIAA J. **32**, 2108 (1994).

[3]S. Zhang and S. P. Schneider, "Molecular-mixing measurements and turbulent-structure visualizations in a round jet with tabs," AIAA Paper No. 94-3082, 1994.

[4]D. Bohl and J. Foss, "Enhancement of passive mixing tabs by the addition of secondary tabs," AIAA Paper No. 96-0545, 1996.

[5]K. B. M. Q. Zaman, M. F. Reeder, and M. Samimy, "Control of an axisymmetric jet using vortex generators," Phys. Fluids A **6**, 778 (1994).

[6]M. F. Reeder and M. Samimy, "The evolution of a jet with vortex-generating tabs: Visualization and analysis of mean and instantaneous properties," J. Fluid Mech. **311**, 73 (1996).

[7]K. B. M. Q. Zaman, "Spreading characteristics and thrust of jets from asymmetric nozzles," AIAA Paper No. 96-0200, 1996.

[8]G. Brown and A. Roshko, "The effect of density difference on the turbulent mixing layer," J. Fluid Mech. **64**, 775 (1974).

[9]S. C. Crow and F. H. Champagne, "Orderly structures in jet turbulence," J. Fluid Mech. **48**, 547 (1971).

[10]K. B. M. Q. Zaman and A. K. M. F. Hussain, "Vortex pairing in a circular jet under controlled excitation. Part 1. General jet response," J. Fluid Mech. **101**, 449 (1980).

[11]G. Raman, E. J. Rice, and E. Reshotko, "Control of an axisymmetric turbulent jet by multi-modal excitation," Proceedings of the 8th Symposium on Turbulent Shear Flows, Technical University of Munich, Vol. 1, p. 6-2, 9–11 September 1991.

[12]G. Raman and E. J. Rice, "Axisymmetric jet forced by fundamental and subharmonic tones," AIAA J. **29**, 1114 (1991).

[13]R. E. Kelly, "On the stability of an inviscid shear layer which is periodic in space and time," J. Fluid Mech. **27**, 657 (1967).

[14]R. R. Mankbadi, "On the interaction between fundamental and subharmonic instability waves in a turbulent round jet," J. Fluid Mech. **188**, 385 (1985).

[15]C.-M. Ho and L. S. Huang, "Subharmonic and vortex merging in mixing layers," J. Fluid Mech. **119**, 443 (1982).

[16]H. S. Husain and F. Hussain, "Experiments on subharmonic resonance in a shear layer," J. Fluid Mech. **304**, 343 (1995).
[17]K. B. M. Q. Zaman, "Axis switching and spreading of an asymmetric jet: The role of coherent structure dynamics," J. Fluid Mech. **316**, 1 (1996).
[18]J. H. Bell and R. D. Mehta, "Measurements of the streamwise vortical structures in a plane mixing layer," J. Fluid Mech. **239**, 213 (1992).
[19]F. K. Browand and J. Laufer, "The role of large-scale structures in the initial development of circular jets," Proceedings of the Turbulence In Liquids Conference, University of Missouri-Rolla, 1975, Vol. 4, pp. 333–344.
[20]C.-M. Ho and E. Gutmark, "Vortex induction and mass entrainment in a small-aspect-ratio elliptic jet," J. Fluid Mech. **179**, 383 (1987).
[21]F. Hussain and H. S. Husain, "Elliptic jets. Part 1. Characteristics of unexcited and excited jets," J. Fluid Mech. **208**, 257 (1989).
[22]F. F. Grinstein, E. J. Gutmark, T. P. Parr, D. M. Hanson-Parr, and U. Obeysekare, "Streamwise and spanwise vortex interaction in an axisymmetric jet. A computational and experimental study," Phys. Fluids **8**, 1515 (1996).